Loop-Directed Mutagenesis of the Blue Copper Protein Amicyanin from *Paracoccus versutus* and Its Effect on the Structure and the Activity of the Type-1 Copper Site

Christian Buning,[†,§] Gerard W. Canters,*[,†] Peter Comba,[†,§] Christopher Dennison,[†,‡] Lars Jeuken,[†] Michael Melter,[†,§] and Joann Sanders-Loehr[||]

Contribution from the Leiden Institute of Chemistry, Leiden University, Gorlaeus Laboratories, 2300 RA Leiden, The Netherlands, and the Department of Biochemistry and Molecular Biology, Oregon Graduate Institute of Science and Technology, Portland, Oregon 97291-1000

Received August 5, 1999

Abstract: Four loop-mutants of the blue copper protein amicyanin from *Paracoccus versutus* have been constructed and characterized. The mutations replaced the loop containing three (Cys93, His96, Met99) of the four copper ligands in amicyanin by the "ligand loops" of *P. aeruginosa* azurin (AmiAzu), *A. faecalis* pseudoazurin (AmiPaz), *P. nigra* plastocyanin (AmiPcy), and *P. aureofaciens* nitrite reductase (AmiNiR). The copper centers of all variants appear to be perfect type-1 Cu sites although the AmiNiR variant exhibits diminished stability. The optical spectra of the AmiAzu and AmiPaz variants display a significant dependence on temperature. Excitation at 457 nm as well as 647 nm results in similar resonance Raman spectra. The reduction potentials of the three stable variants are all higher than that of *wt* amicyanin. The reduced forms of the loop-mutants protonate at the C-terminal histidine, with pK_a values of 5.6 (AmiAzu), 5.4 (AmiPaz), and 5.7 (AmiPcy) (6.8 for *wt* amicyanin). AmiAzu is the first known cupredoxin with more than two amino acids between the cysteine and histidine ligands that undergoes this protonation. The electron self-exchange rate constants at 25 °C are 5.7−7.5 times lower for the loop mutants than for *wt* amicyanin (1.2×10^5 M^{-1} s^{-1}). The results are interpreted by taking into consideration that three metal ligands are intimately connected with the stable β-sandwich structure of the cupredoxin. This leaves considerable freedom in positioning the fourth one, the C-terminal His, on the "ligand loop". This explains the ease by which the C-terminal histidine ligand can be excised and replaced by external ligands without losing the metal binding property of the protein. The results also help understand the remarkable evolutionary success of the combination of cupredoxin fold and Cu site for mediating biological electron transfer.

Introduction

Whenever nature uses copper to promote biological electron transfer (ET), the metal appears to be encased in what has come to be known as the cupredoxin fold.[1] The question why this combination of metal site and fold is such a unique and successful vehicle for biological ET is addressed in this paper. The fold is usually made up of 6−8 β-strands in a Greek key folding motif. The strands arrange themselves into two β-sheets which face each other to form a β-sandwich.[1] Within a cupredoxin domain the so-called type-1 copper binding site is located excentrically at a distance of 5−7 Å from the outer surface. The metal is anchored in the protein structure by strong bonds to three ligands, a cysteine and two histidines which coordinate by their S^{γ}-atom and their N^{δ}-atoms, respectively, in a trigonal planar or a trigonal pyramidal geometry. A weaker fourth ligand, consisting of a methionine or, sometimes, a glutamine, coordinating with its S^{δ}- or O^{ϵ}-atom, respectively, occupies the axial position (see Figure 1).[2] In some cases (azurins) a second weakly interacting axial group in the form of a backbone carbonyl oxygen is found at the opposite axial position.[3]

Cupredoxin domains also occur as part of multicopper, multidomain enzymes. Examples are the blue oxidases (laccase,[4] ascorbate oxidase,[5] and ceruloplasmin[6]) and nitrite reductase (NiR).[7−10] Again the copper in the ET site is bound to a cysteine and two histidines, while a methionine, leucine, or phenylalanine may occupy the fourth (axial) position. A stunning illustration of the versatility of the cupredoxin fold, when it comes to

[†] Leiden University.
[§] Present address: Anorganisch-Chemisches Institut der Universität Heidelberg, Im Neuenheimer Feld 270, 69120 Heidelberg, Germany.
[‡] Present address: Department of Chemistry, University of Newcastle, Newcastle upon Tyne, NE1 7RU, U.K.
[||] Oregon Graduate Institute of Science and Technology.

(1) Adman, E. T. *Adv. Protein Chem.* **1991**, *42*, 144−197.
(2) Romero, A.; Nar, H.; Huber, R.; Messerschmidt, A.; Kalverda, A. P.; Canters, G. W.; Durley, R.; Mathews, P. S. *J. Mol. Biol.* **1994**, *236*, 1196−1211.
(3) (a) Nar, H.; Messerschmidt, A.; Huber, R.; van de Kamp, M.; Canters, G. W. *J. Mol. Biol.* **1991**, *221*, 765−772. (b) Baker, E. N. *J. Mol. Biol.* **1988**, *203*, 1071−1095.
(4) Ducros, V.; Brzozowski, A. M.; Wilson, K. S.; Brown, S. H.; Ostergaard, P.; Schneider, P.; Yaver, D. S.; Pedersen, A. H.; Davies, G. J. *Nat. Struct. Biol.* **1998**, *5*, 310−316.
(5) Messerschmidt, A. *Adv. Inorg. Chem.* **1993**, *40*, 121−185.
(6) Zaitseva, I.; Zaitseva, V.; Acrol, G.; Moshrov, K.; Bax, B.; Ralph, A.; Windley, Z. P. *J. Biol. Inorg. Chem.* **1996**, *1*, 15−23.
(7) Murphy, M. E. P.; Turley, S.; Adman, E. T. *J Biol. Chem.* **1997**, *272*, 28455−28460.
(8) Adman, E. T.; Godden, J. W.; Turley, S. *J. Biol. Chem.* **1995**, *270*, 27458−27474.
(9) Inoue, T.; Gotowda, M.; Deligeer; Kataoka, K.; Yamaguchi, K.; Suzuki, S.; Watanabe, H.; Gohow, M.; Kai, Y. *J. Biochem.* **1998**, *124*, 876−879.
(10) Dodd, F. E.; Van Beeumen, J.; Eady, R. R.; Hasnain, S. S. *J. Mol. Biol.* **1998**, *282*, 369−382.

10.1021/ja992796b CCC: $19.00
Published on Web 12/31/1999

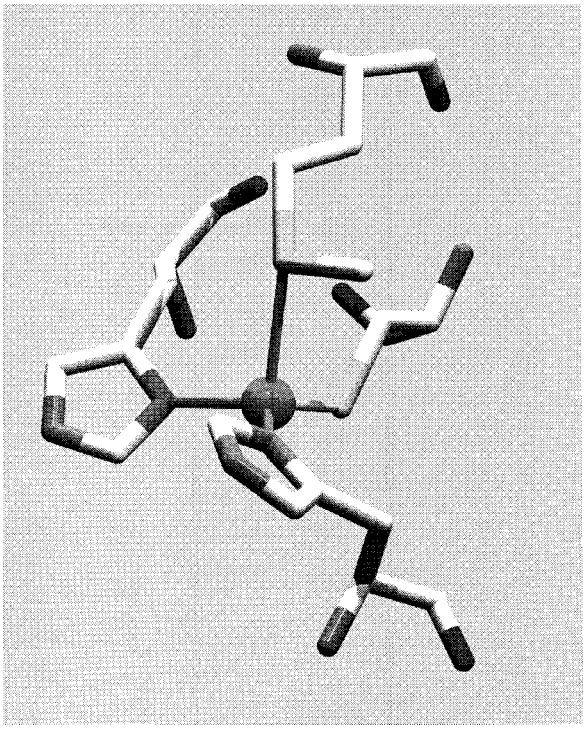

Figure 1. Active-site structure of *wt* amicyanin (*Paracoccus versutus*).[2,27]

incorporating copper, is provided by subunit II (SUII) of cytochrome oxidase.[11] Its cupredoxin domain harbors a dinuclear copper center (Cu_A site) that can be considered as two joint type-1 sites. Each copper center is coordinated in-plane to two bridging cysteines and a histidine. The axial ligand is different for the two copper ions, i.e., a methionine for one copper and a backbone carbonyl oxygen for the other one.

From an inorganic chemist's point of view the structure of the type-1 site is "unnatural" in the sense that it deviates from the structures which are familiar from the coordination chemistry of small Cu(I) and Cu(II) coordination compounds (tetrahedral and square planar/octahedral, respectively). Since it requires energy to deform such a geometry to a type-1 site geometry, the latter has been considered as being strained.[12,13] Presumably, a type-1 copper site is kept in this conformation by the surrounding protein matrix. Building on ideas formulated initially by Pauling with respect to enzymatic catalysis[14] and later elaborated by Lumry and Eyring,[15] Vallee and Williams[16] and Malmström and co-workers[13] have assigned a mechanistic significance to this strained state: as the structure of a type-1 site is intermediate between those of Cu(I) and Cu(II) (frozen transition state or "entatic state"[12,16]), the site appears ideally suited to its physiological role: the shuttling of electrons. The protein structure, thus, is conceived of as a delicately built scaffold ("rack"[13]) that poises the metal to perform its function as efficiently as possible with minimal reorganizational energy. Another property that has been connected with the geometry of type-1 sites is the redox potential. It has been argued that the structure of the type-1 site plays an important role in raising the redox potential considerably above the Cu(I)/Cu(II) couple in water.[12,13]

A striking feature of the metal binding site in all cupredoxin domains is that only one of the metal ligands (a histidine) is located on a β-strand inside the protein framework, while all the other ligands (three for a type-1 site and five for a Cu_A site) invariably are located outside the protein core and are found on a single, C-terminally located loop connecting two β-strands. These loops show great variability in composition and length (see Table 1) and apparently are tailored to the individual β-sandwich to which they are attached. We thought it of interest to see if different loops could be grafted onto the same framework (for instance, that of amicyanin) and to see if stable metal binding sites would be obtained. In this way it might be possible to check experimentally to what extent the individual type-1 sites in the cupredoxin fold are unique. The experiments might also shed light on the question to what extent the properties of a site are determined by the loop and to what extent by the protein core. A preliminary loop-directed mutagenesis experiment along these lines was reported earlier[17] while related experiments dealing with the Cu_A loop of cytochrome oxidase have been reported elsewhere.[18,19]

By performing these experiments another issue could also be addressed. In a number of blue copper proteins, including pseudoazurin,[20,21] plastocyanin,[22,23] and amicyanin,[24] the histidine located on the "ligand loop" is known to be protonatable when the copper is in the reduced state. The concomitant huge rise in redox potential effectively abolishes the redox activity of the protein.[17,25] It has been proposed for plastocyanin that this may constitute a metabolic feed-back mechanism [see ref 26 and references contained therein]: a high rate of photosynthesis induces a drop in pH and, consequently, a drop in the activity of the blue copper protein. The photosynthetic rate then would slow. The composition and length of the C-terminal loop have been correlated with the titration behavior of this C-terminal histidine ligand.[20] The experiments to be described here have also been used to test this hypothesis.

In the present work the loops of three blue copper proteins (azurin, pseudoazurin, and nitrite reductase) have been fused onto the framework of the blue copper protein amicyanin by means of loop-directed mutagenesis. The results are discussed together with the results of an earlier study by which the active site loop of plastocyanin was introduced into amicyanin[17] and the amicyanin variant $H^{96}PFM^{99} \rightarrow H^{96}QGAGM^{101}$ (AmiPcy) was obtained. Figure 2 shows the loop structure of amicyanin from *Paracoccus versutus*[2,27] (Ami) and the loop structures of

(11) (a) Tsukihara, T.; Aoyama, H.; Yamashita, E.; Tomizaki, T.; Yamaguchi, H.; ShinzawaItoh, K.; Nakashima, R.; Yaono, R.; Yoshikawa, S. *Science* **1996**, *272*, 1136−1144. (b) Blackburn, N. J.; deVries, S.; Barr, M. E.; Houser, R. P.; Tolman, W. B.; Sanders, D.; Fee, J. A. *J. Am. Chem. Soc.* **1997**, *119*, 6135−6143. (c) Iwata, S.; Ostermeier, C.; Ludwig, B.; Michel, H. *Nature* **1995**, *376*, 660−669. (d) Wilmanns, M.; Nappalainen, P.; Kelly, M.; Sauer-Erikson, E.; Saraste, M. *Proc. Natl. Acad. Sci. U.S.A.* **1995**, *92*, 11955−11959.

(12) Williams, R. J. P. *Eur. J. Biochem.* **1995**, *234*, 363−381.

(13) Malmström, B. G. *Eur. J. Biochem*. **1994**, *223*, 711−718.

(14) Pauling, L. *Nature* **1948**, *161*, 707−709.

(15) Lumry, R.; Eyring, H. *J. Phys. Chem*. **1954**, *58*, 110−120.

(16) Vallee, B. L.; Williams, R. J. P. *Proc. Natl. Acad. Sci. U.S.A.* **1968**, *59*, 498−505.

(17) Dennison, C.; Vijgenboom, E.; Hagen, W. R.; Canters, G. W. *J. Am. Chem. Soc.* **1996**, *118*, 7406−7407.

(18) Dennison, C.; Vijgenboom, E.; de Vries, S.; van der Oost, J.; Canters, G. W. *FEBS Lett.* **1995**, *365*, 92−94.

(19) Hay, M.; Richards, J. H.; Lu, Y. *Proc. Natl. Acad. Sci. U.S.A.* **1996**, *93*, 461−464.

(20) (a) Dennison, C.; Kohzuma, T.; McFarlane, W.; Suzuki, S.; Sykes, G. A. *J. Chem. Soc., Chem. Commun.* **1994**, 581−582. (b) Dennison, C.; Kohzuma, T.; McFarlane, W.; Suzuki, S.; Sykes, G. A. *Inorg. Chem.* **1994**, *33*, 3299−3305.

(21) Vakoufari, E.; Wilson, K. S.; Petratos, K. *FEBS Lett.* **1994**, *347*, 203−206.

(22) Markley, J. L.; Ulrich, E. I.; Berg, S. P.; Krogmann, D. W. *Biochemistry* **1975**, *14*, 4428−4433.

(23) Guss, J. M.; Harrowell, P. R.; Murata, M.; Norris, V. A.; Freeman, H. C. *J. Mol. Biol.* **1986**, *192*, 361−387.

(24) Lommen, A.; Canters, G. W. *J. Biol. Chem.* **1990**, *265*, 2768−2774.

(25) Sykes, A. G. *Adv. Inorg. Chem.* **1991**, *36*, 377−408.

Table 1. Amino Acid Sequences of the C-Terminal Ligand-Containing Loops of Several Type-1 Blue Copper Centers[f]

protein	sequence of the C-terminal loops													
Amicyanin[a]	**Cys**	Thr						Pro		**His**	Pro			Phe	**Met**
Plastocyanin[b]	**Cys**	Ser						Pro		**His**	Gln	Gly	Ala	Gly	**Met**
Pseudoazurin[c]	**Cys**	Thr						Pro		**His**	Tyr	Ala	Met	Gly	**Met**
Azurin[d]	**Cys**	Thr	Phe					Pro	Gly	**His**	Ser		Ala	Leu	**Met**
NiR[e]	**Cys**	Ala	Pro	Gln	Gly	Met	Val	Pro	Trp	**His**	Val	Val	Ser	Gly	**Met**

[a] *Paracoccus versutus.* [b] *Populus nigra.* [c] *Alcaligenes faecalis.* [d] *Pseudomonas aeruginosa.* [e] *Pseudomonas aureofaciens.* [f] In all cases the ligands are in bold.

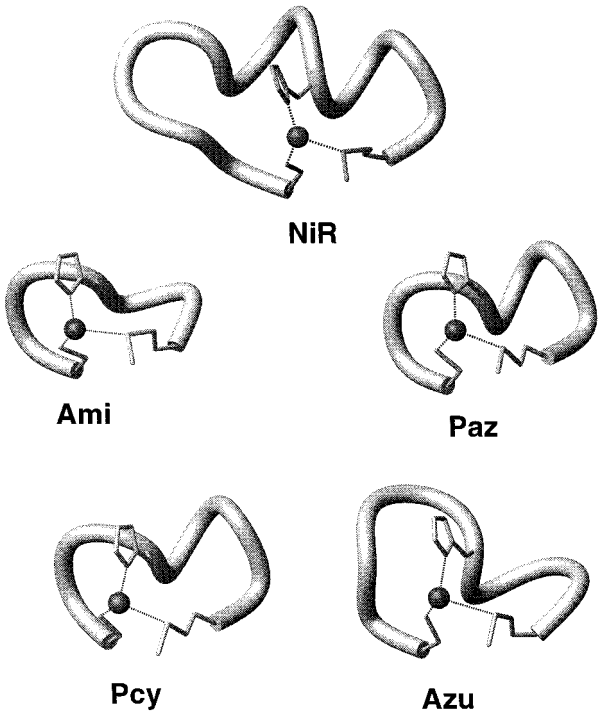

Figure 2. C-terminal loops of amicyanin (*Paracoccus versutus*) (Ami), plastocyanin (*Populus nigra*) (Pcy), azurin (*Alcaligenes denitrificans*) (Azu), pseudoazurin (*Alcaligenes faecalis*) (Paz), and nitrite reductase (*Alcaligenes xylosoxidans*) (NiR).

the *wt* proteins from which the inserts originate (Pcy, plastocyanin from *Populus nigra*;[23,28] Azu, azurin from *Pseudomonas aeruginosa*;[3,29] Paz, pseudoazurin from *Alcaligenes faecalis*;[21,30] NIR, nitrite reductase from *Alcaligenes xylosoxidans*[10]). (The loop inserted in AmiNiR derives from *P. aureofaciens.* Since no structure is available of this NiR the loop of the homologous *A. xylosoxidans* was used for Figure 2). Of special interest is the question whether a stable copper binding site is obtained in all these cases and what the spectroscopic features of each site can tell us about its structure. The activity of the protein has been assessed by establishing its redox potential and its electron self-exchange rate constant. The pK_a of the histidine located on the "ligand loop" has been determined by NMR.

Materials and Methods

Proteins. The mutation $C^{93}TPH^{96}PFM^{99} \rightarrow C^{93}TFPGH^{98}SALM^{102}$ (*AmiAzu*) was performed with a modified version of the unique site elimination protocol[31] while the $C^{93}TPH^{96}PFM^{9} \rightarrow C^{93}TPH^{96}YAMGM^{101}$ (*AmiPaz*) and $C^{93}TPH^{96}PFM^{99} \rightarrow C^{93}APQGMVPWH^{102}VVSGM^{107}$ (*AmiNiR*) mutations were carried out with a method based on two consecutive PCR reactions. DNA sequencing verified the mutations in all cases. The plasmid pUC18 was used as a cloning vector, with the gene coding for the mutants under control of the *lac* promoter. The plasmids containing the genes encoding AmiAzu and AmiPaz were transformed into JM101 and expression and isolation were carried out as described previously.[32]

The plasmid containing the *AmiNiR* mutant was transformed in BL21. Expression and isolation were carried out as described[32] with one modification: instead of binding the protein to the CM column, the protein was bound to phenyl-sepharose (Pharmacia) after adding ammonium sulfate to an end-concentration of 1.5 M. The protein was eluted using a gradient from 1 to 0 M NH_4SO_4 (25 mM phosphate, pH 7.0). Protein fractions were collected, concentrated to about 1 mL using ultra-filtration, and further purified using a gel-filtration (Superdex 75, Pharmacia) column. Due to instability the final yield was ~0.3 mg L^{-1} of cell culture.

EPR Spectroscopy. X-band EPR spectra were recorded at 77 K on a JEOL JESRE2X spectrometer (~9 GHz) unless mentioned otherwise. The program JEOL ESPRIT330 was used for data manipulation. DPPH (diphenylpicrylhydrazine) was used as an external reference. To record the spectra of AmiAzu, AmiPaz and AmiNiR glycerol (end concentration of 30−40%) were added to a 10 mM *N*-[2-hydroxyethyl]piperazine-*N*′-[2-ethanesulfonic acid] (HEPES), pH 7, solution of the protein in water. For spectral simulations the programs SIMFONIA[33] (AmiAzu) and KOPER[34] (AmiPaz, AmiNiR) were used. EPR spectra in the temperature range of 100−250 K were recorded on glycerol−water (2:1) samples with a Bruker ESP300E instrument. Spectra were simulated with the EPR50f software.

Electronic Spectroscopy. UV/vis spectra were recorded on a Shimadzu UV-2101PC spectrophotometer (25 °C; 10 mM HEPES; pH 7). Low-temperature UV/vis spectra were recorded on a homemade spectrophotometer provided with a liquid helium cryostat. For the low-temperature optical experiments the samples of AmiPaz (3 mM in 20 mM HEPES, pH 7) and AmiAzu (3 mM in 5 mM HEPES, pH 7) were diluted prior to the measurement by adding glycerol to a final content of 66% glycerol.

^{1}H NMR Spectroscopy. ^{1}H NMR spectra were recorded at 25 °C on Bruker WM300, DMX600 ,and Varian Unity 500 spectrometers. Protein samples were reduced by adding aliquots of 0.1 M sodium dithionite made up in 0.1 M NaOH, or 0.1 M sodium ascorbate. For electron self-exchange rate measurements the proteins were exchanged, using ultrafiltration (Amicon, 5kD membrane), into 99.95% deuterated 18 mM phosphate buffer at pH 8.2 (I = 0.05 M). This procedure automatically took care of the removal of excess reductant. Measurements were also carried out on the AmiAzu variant in 22 mM phosphate buffer at pH 7.2 (I = 0.05 M). The reduced protein was transferred to an NMR tube and flushed with argon. Fully oxidized protein was obtained by the addition of aliquots of 0.1 M $K_3[Fe(CN)_6]$; excess oxidant was removed by ultrafiltration.

For the determination of the electron self-exchange rate constant NMR spectra were obtained of the reduced protein containing various

(26) Jackman, M. P.; Sinclair-Day, J. D.; Sisley, M. J.; Sykes, A. G.; Denys, L. A.; Wright, P. E. *J. Am. Chem. Soc.* **1987**, *109*, 6443−6449.
(27) Kalverda, A. P.; Wymenga, S. S.; Lommen, A.; van de Ven, F. J.; Hilbers, C. W.; Canters, G. W. *J. Mol. Biol.* **1994**, *240*, 358−371.
(28) Guss, J. M.; Bartunik, H. D.; Freeman, H. C. *Acta Crystallogr. B* **1992**, *48*, 790−811.
(29) Adman, E. T.; Jensen, L. H. *Isr. J. Chem.* **1981**, *21*, 8−12.
(30) Petratos, K.; Dauter, Z.; Wilson, K. S. *Acta Crystallogr. B* **1988**, *44*, 628−636.
(31) Deng, W. P.; Nickoloff, J. A. *Anal. Biochem.* **1992**, *260*, 81−88.
(32) Kalverda, A. P.; Salgado, J.; Dennison, C.; Canters, G. W. *Biochemistry* **1996**, *35*, 3085−3092.
(33) WIN-EPR SimFonia, GmbH.; Version 1.25; Copyright 1994−1996.
(34) Hagen, W. R. *Advanced Electron Paramagnetic Resonance Spectral Simulator*; Main program KOPER, version 3.11 (960102); Copyright W. R. Hagen 910116. All rights reserved. 1991.

amounts of the oxidized protein. The concentration of oxidized protein present was determined by transferring the NMR sample to a 1 or 2 mm path length UV/vis cuvette and determining the absorbance at the appropriate wavelength. The concentration of oxidized protein was determined before and after the measurement of the NMR spectrum and the average was used in the calculations. The effect of increasing concentrations of oxidized protein on the line width of the resolved imidazole ring resonances of the two histidine ligands was measured. The self-exchange rate constant, k_{ese}, was obtained from the slope of plots of the exchange-induced line broadening, ΔT_2^{-1}, against the concentration of oxidized protein [Ox]:[35] $\Delta T_2^{-1} = k_{ese}[\mathrm{Ox}]$.

The effect of pH on the Cu(I) form of the loop variants was studied on solutions of the proteins in 20 mM phosphate (99.95% D_2O). The sample was flushed with argon in an NMR tube and reduced by using aliquots of 0.1 M sodium dithionite in 0.1 M NaOD. To prevent reoxidation of the sample a small amount of ascorbic acid was added to the protein solution. The concentration of the reduced protein was approximately 2 mM. The pH of the sample was adjusted with 0.1 M NaOD or 0.1 M DCl. The quoted pH values of the NMR samples have not been corrected for the deuterium isotope effect.

Electrochemistry. Cyclic voltammetry measurements were carried out at room temperature, using an Autolab potentiostat (Eco Chemie, Holland), with either a glassy carbon disk working electrode or a mercaptopyridine treated gold working electrode, a standard calomel electrode as a reference, and a platinum counter electrode as described previously.[36] The sample concentration was 1−2 mg/mL and measurements were carried out at pH 8.0 (20 mM *N*-tris[hydroxymethyl]methyl-2-aminoethanesulfonic acid (TES)), pH 7.0 (20 mM HEPES), 6.0, 5.5, and 5.0 (20 mM 2-[*N*-morpholino]ethanesulfonic acid (MES)) all at $I = 0.10$ M (NaCl). The peak separation was 100 ± 10 mV for AmiAzu and 76 ±10 mV for AmiPaz. All potentials are referenced to NHE.

Redox Titrations. Redox titrations of the reduced mutants with potassium ferricyanide were performed in 0.10 M potassium phosphate, pH 7.0, at 298 K.[37] Analyses of the data were performed with a slightly modified form of a published equation, yielding the midpoint potential and the optical extinction of the 600 nm absorption band.[37,38]

Raman Spectroscopy. Raman spectra were obtained on a McPherson 2061/207 spectrograph (0.67 m, 2400-groove grating) using a Kaiser Optical holographic supernotch filter and a Princeton Instruments (LN-1100PB) liquid N_2-cooled CCD detector. Excitation was provided by Coherent Innova 302 Kr (647.1 nm) or Innova 90 Ar (457.9 nm) lasers using 70 mW power, 4 cm^{-1} spectral resolution, and 30 min data accumulation. Spectra were collected in a 150° backscattering geometry from samples maintained at 15−200 K by use of a closed-cycle helium refrigerator (Air Products Displex).[39] Absolute peak frequencies were calibrated relative to aspirin and CCl_4 and are accurate to ±1 cm^{-1}. Relative peak frequencies in spectra recorded under identical experimental conditions are accurate to ±0.5 cm^{-1}.

Results

Electronic Spectra. AmiPcy, AmiAzu, and AmiPaz are stable metalloproteins, while AmiNiR has a labile copper center. The latter observation may have to do with the occurrence of an alanine in the amino acid sequence of the AmiNir variant following the ligand cysteine (see Table 1). Usually a Thr or Ser is found at this position. The stabilizing influence of these residues on the network of H-bonds around the copper center has been noted before.[1,3b,40,41] The visible spectra of *wt* amicyanin and of the four loop mutants are shown in Figure 3, while the numerical data are given in Table 2. In previous studies the ∼460 nm absorption band, like the band at 600 nm, has been assigned to a S(Cys) → Cu(II) LMCT transition.[39,42] Increased absorption at ∼460 nm often is accompanied by an increased rhombicity in the EPR spectrum.[39,42,43] The loop elongation in the case of *AmiAzu* results in a copper site with a A_{467}/A_{608} ratio of 0.19, compared to $A_{460}/A_{596} = 0.10$ for *wt* amicyanin. In *AmiPaz* an even larger A_{460}/A_{593} ratio of 0.28 is found (similar to the A_{460}/A_{592} ratio of 0.26 for *AmiPcy*[17]). The visible spectrum of the *AmiNiR* loop mutant is similar to that of *wt* amicyanin with a A_{459}/A_{598} ratio of 0.12. For AmiAzu and AmiPaz the $A_{\sim460}/A_{\sim600}$ ratio is temperature dependent. This effect is most pronounced in AmiPaz where the ratio increases to 0.60 at 4 K (note that there is also a temperature-dependent change of the absorption bandwidth; see Figure 4).

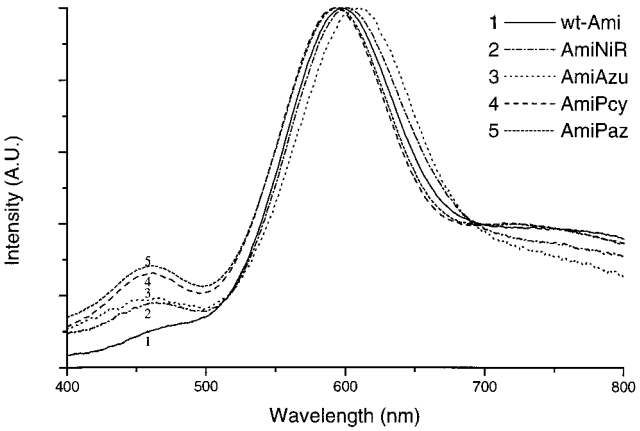

Figure 3. Electronic spectra of the loop mutants: absorbance (arbitrary units) vs wavelength (nm). Spectra were normalized to the maxima of their absorptions around 600 nm. $T = 25$ °C; 20 mM Hepes, pH 7.

EPR Spectra. The EPR spectra of the *AmiAzu* and *AmiPaz* mutants are rhombic, like the spectrum of the *AmiPcy* variant (see Figure 5).[17] The EPR spectrum of the *AmiNiR* loop mutant is axial, like that of *wt* amicyanin (see Figure 5). The *g* and *A* values obtained from simulations of these spectra are listed in Table 2. All of the spectra shown in Figure 5 have typically small hyperfine coupling constants in the g_z region (A_z). The spectra do not show a change with temperature in the range of 100 to 200 K except for some line broadening at elevated temperatures.

pH Titrations of Reduced Proteins Studied by ^{1}H NMR. The chemical shifts of the resonances of the $C^{\epsilon1}$ and $C^{\delta2}$ protons of the C-terminal histidine were used to monitor its pH titration behavior. Both for reduced AmiAzu and AmiPaz this histidine (which is one of the four copper ligands) protonates at low pH, as indicated by a downfield shift of the imidazole ring protons (data not shown). The $C^{\epsilon1}H$ signal was assigned based on its larger shift upon protonation of the histidine and was used for the determination of pK_a values (see Table 2).

Reduction Potentials. The reduction potentials of the various loop mutants of amicyanin (except AmiNiR) were determined from pH 5 to 8 by cyclic voltammetry, although the data below pH 6 had a diminished signal-to-noise ratio and are less reliable. Also redox titrations were performed with the $[Fe(CN)_6]^{3-/4-}$

(35) (a) Leigh, J. S., Jr. *J. Magn. Reson.* **1971**, *4*, 308−311. (b) Johnston, E. R.; Grant, D. M. *J. Magn. Reson.* **1982**, *47*, 282−291. (c) Groeneveld, C. M.; Canters, G. W. *J. Biol. Chem.* **1988**, *203*, 167−173.
(36) Hagen, W. R. *Eur. J. Biochem.* **1980**, *182*, 523−530.
(37) van de Kamp, M.; Silvestrini, M. C.; Brunori, M.; van Beeumen, J.; Hali, F. C.; Canters, G. W. *Eur. J. Biochem.* **1990**, *194*, 109−118.
(38) Goldberg, M.; Pecht, I. *Biochemistry* **1976**, *15*, 4197−4208.
(39) Han, J.; Loehr, T. M.; Lu, Y.; Valentine, J. S.; Averill, B. A.; Sanders-Loehr, J. *J. Am. Chem. Soc.* **1993**, *115*, 4256−4263.
(40) Hoitink, C. W.; Canters, G. W. *J. Biol. Chem.* **1992**, *20*, 13836−13842.
(41) Dong, S.; Ybe, J. A.; Hecht, M. H.; Spiro, T. G. *Biochemistry* **1999**, *38*, 3379−3385.
(42) LaCroix, L. B.; Shadle, S. E.; Wang, Y. N.; Averill, B. A.; Hedman, B.; Hodgson, K. O.; Solomon, E. I. *J. Am. Chem. Soc.* **1996**, *118*, 7755−7768.
(43) Pierloot, K.; De, K. J.; Ryde, U.; Olsson, M. H. M.; Roos, B. O. *J. Am. Chem. Soc.* **1998**, *120*, 13156−13166.

Table 2. Properties of the Loop Mutants of Amicyanin (AmiPcy, AmiAzu, AmiPaz, AmiNiR) and Those of the Corresponding Native Copper Proteins (n/d = not determined)

parameter	Amicyanin[a]	Plastocyanin[b]	Ami-Pcy[c]	Azurin[d]	Ami-Azu[q]	Pseudo-azurin[e]	Ami-Paz[q]	Blue NiR[f]	Green NiR[g]	Ami-NiR[q]
Cu plane [Å]	0.40	0.36		0.08		0.43		*0.5*	~0.4	
Cu−S(Met) [Å]	2.84	2.82		3.12		2.76		*2.62*	2.56[m]	
$\lambda_{max,1}$ [nm]	460	460	460	481	467	450	460	474	458	459
$\lambda_{max,2}$ [nm]	596	597	592	628	608	593	593	595	585	598
$\epsilon_{\sim 600}$ [$mM^{-1}\,cm^{-1}$]	3.9	4.8	3.9	5.7	4.1	2.9	4.0	7.0	1.9	n.d.
$A_{\sim 460}/A_{\sim 600}$[h]	0.10	0.06	0.26	0.04	0.19	0.41	0.28	0.21	1.34	0.12
EPR[i]	ax	ax	rh	ax	rh	rh	rh	ax	rh	ax
g_x	2.046	2.053	2.017	2.035[n]	2.015	*2.01*	2.022	2.045		2.045
g_y			2.041	2.051	2.041	*2.09*	2.060			
g_z	2.239	2.226	2.204	2.276	2.233	*2.21*	2.215	2.218	*2.19*	2.220
A_x [mT]			6.9		7.6		6.9			-
A_y [mT]					1.1					-
A_z [mT]	5.6	6.3	4.3	5.1	2.7	*5.0*	3.8	6.4	*6.6*	5.0
ν(Cu−S) [cm^{-1}][j]	409	408	402	414	397	381	400		375	
pK_a[k]	6.8	4.7	5.71		5.63	*4.84*	5.4			
$E°_{tit}$ [mV] (pH 7)	260		310	319	298	270	283			
$E°_{cv}$ [mV] (pH 7)	248	361	308		296		282		*270*	n/d
k_{ese} [$M^{-1}\,s^{-1}$][l]	1.3×10^5	~10^3[o]	2.1×10^4	8×10^5	1.6×10^4	*2.8×10^3*	1.6×10^4			n/d

[a] *P. versutus*, refs 2, 17, 24, 60, and this work. [b] *Populus nigra*, refs 28, 41, 44, and 61. [c] Reference 17. [d] *P. aeruginosa*, refs 3, 45, 64, 65, and 66, pH 9.0 (except ν(Cu−S) and $E°$). [e] *Alcaligenes faecalis* S-6, refs 30, 39, 44, and 58; *A. cycloclastes* (Italics), refs 20, 67, and 68. [f] *P. aureofaciens*, ref 69; *A. xylosoxidans* (italics), ref 10. [g] *A. cycloclastes*, refs 8 and 39; *A. faecalis* S-6 (italics), refs 58 and 70. [h] Intensity ratio at 298 K. [i] ax = axial, rh = rhombic. [j] Cu−S(Cys) stretch based on weighted average of Raman frequencies of three most intense peaks; data obtained at 15 K using excitation within the 600 nm absorption band, except for *wt* NiR where data were averaged for the 593 and 695 nm absorption bands. [k] For C-terminal histidine ligand. [l] Self-exchange rate constant, pH ~8.0, 298 K. Azurin: 309 K, pH 9.0. [m] Average of multiple structures. [n] EPR of ^{63}Cu at pH 9.2. [o] To our knowledge the k_{ese} of *Populus nigra* plastocyanin has not been determined. The quoted value refers to spinach plastocyanin. [q] This work.

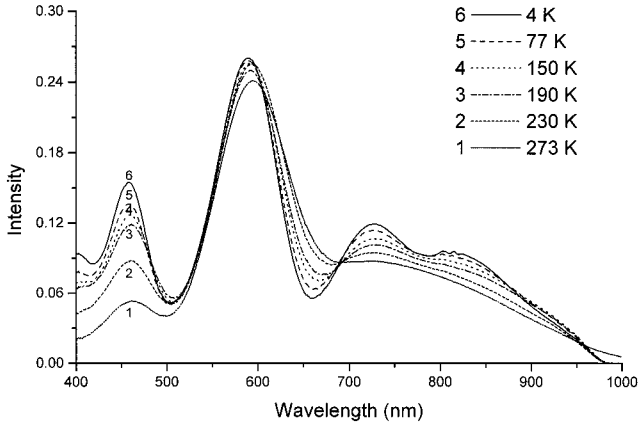

Figure 4. Electronic spectra of AmiPaz (250 μM in 1:2 water−glycerol, 20 mM Hepes, pH 7) at various temperatures (as indicated in the figure).

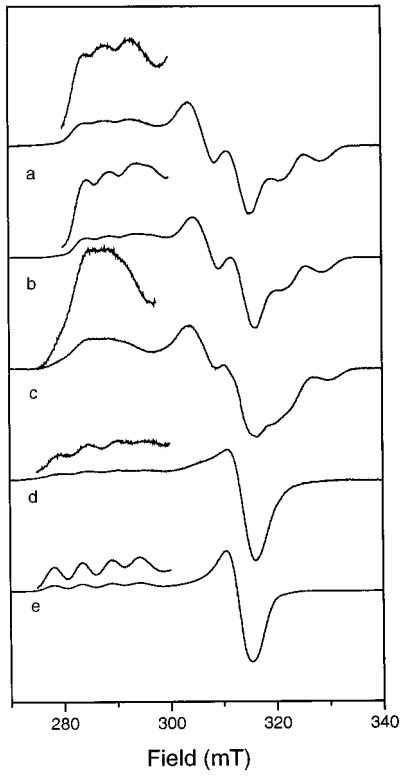

Figure 5. X-band EPR spectra of the loop mutants (1−2 mM in 1:2 water−glycerol, 20 mM Hepes, pH 7) at 77 K; modulation amplitude 0.1 mT: (a) AmiPaz; (b) AmiPcy; (c) AmiAzu; (d) AmiNir; and (e) *wt* Ami. Insets: vertical scale ×4.

couple at pH 7.0 (see Table 2). The values obtained from the two methods agree within 2 mV. The reduction potentials of the loop mutants are higher than that of *wt* amicyanin, by 34−62 mV at pH 7. The reduction potentials increased at pH <7 due to the titration of the histidine in the ligand loop of the reduced protein, similar to what has been observed for *wt* amicyanin.[17] Due to instability of the proteins at low pH at the electrode this could not be investigated in detail.

Electron Self-Exchange Rate Constants. The electron self-exchange rate constant (25 °C), k_{ese}, for the *AmiPaz* loop mutant was determined as 1.6×10^4 M^{-1} s^{-1} (pH 8.2; $I = 0.05$ M). This compares with a k_{ese} of 1.3×10^5 M^{-1} s^{-1} for *wt* amicyanin under identical conditions.[24] The k_{ese} of *AmiAzu* was measured at a lower pH value (7.2) since at pH 8.2 the resonances of His98 were not well enough resolved to allow accurate measurement of peak widths. The k_{ese} of AmiAzu was found to be 1.6×10^4 M^{-1} s^{-1} (pH 7.2, $I = 0.05$ M and 25 °C). The k_{ese} (25 °C) of *AmiPcy* has previously been shown to be 2.1×10^4 M^{-1} s^{-1} (pH 8.2; $I = 0.05$ M).[17] Remarkable about these findings is that the mutants have ese rate constants that are only 5−8 times lower than *wt*, which means that they are still viable electron-transfer catalysts.

Raman Spectroscopy. (a) Effect of *T* and λ_{exc}. The RR spectra for AmiPaz are shown in Figure 6 ($\lambda_{exc} = 457$ nm) and Figure 7B ($\lambda_{exc} = 647$ nm). The spectrum of *wt* amicyanin is

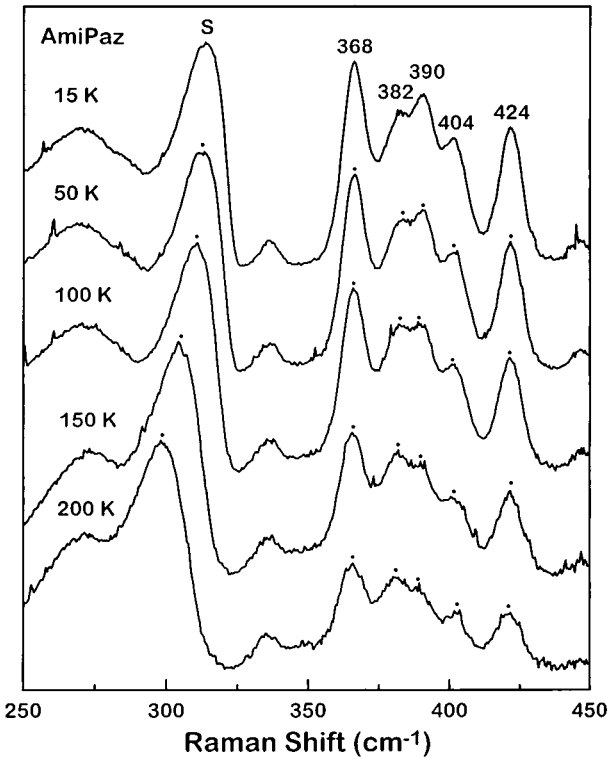

Figure 6. Resonance Raman spectra of AmiPaz under 457 nm excitation at 15, 50, 100, 150, and 200 K (from top to bottom).

reproduced in Figure 7A for comparison. The vibrational frequencies in both spectra (Figures 6 and 7B) are similar while the intensity distributions over the peaks in the two spectra appear to be different. In general RR *frequencies* are determined by the vibrational potential wells in the electronic ground state and are independent of the excitation wavelength, while the *intensities* depend on the origin shift of the excited state with respect to the ground state. These shifts vary with the excited state. Thus, the observations in Figures 6 and 7B confirm that we are dealing with two excited states of one and the same species. The RR transitions are approximately constant in the temperature range of 15−200 K. The increase in RR intensity (relative to ice modes) in going from 200 to 15 K (Figure 6) reflects the increase in absorbance at 457 nm over this same temperature range (Figure 4).

(b) RR Frequencies. The RR spectrum of *AmiPcy* (Figure 7C) is similar both to amicyanin and plastocyanin,[39,44] that is, the most intense transitions occur at 424 cm^{-1}. This peak is assigned to a transition with primarily Cu−S stretching character, based on its high intensity and the ensuing combination bands. The cluster of resonance-enhanced modes between 360 and 450 cm^{-1} gain intensity by kinematic coupling of Cu−S stretching with cysteine ligand deformations. The band positions and intensities in this cluster are closer to those of amicyanin than those of plastocyanin. In the RR spectrum of AmiPcy, each of the peaks in the cluster of resonance-enhanced modes shifts by −1 to −2 cm^{-1} relative to the Raman spectrum of *wt* amicyanin. In addition, there is an increase in intensity at 389 cm^{-1} with a corresponding decrease in intensity at 403 and 424 cm^{-1}.

The Raman spectrum of *AmiPaz* (Figure 7B) is almost identical with that of AmiPcy with respect to both band positions and intensities. The Raman pattern of AmiPaz is definitely closer

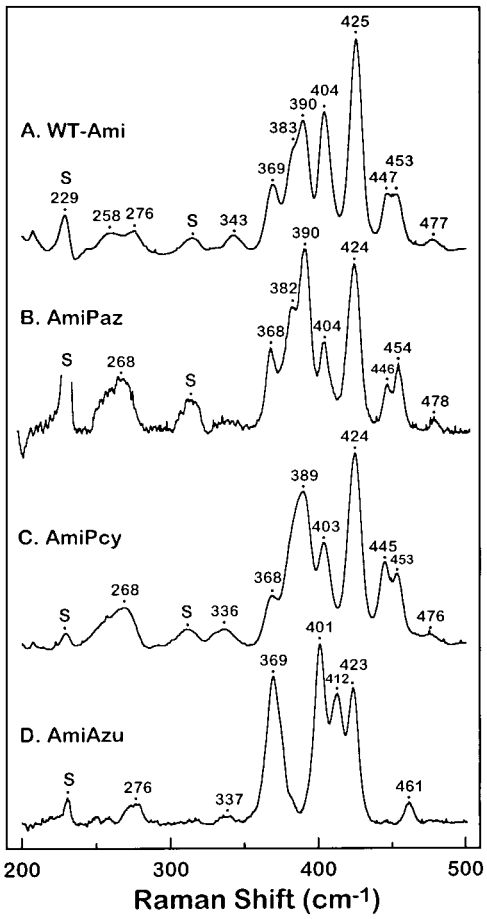

Figure 7. Resonance Raman spectra of *wt* amicyanin, AmiPaz, AmiPcy, and AmiAzu (from top to bottom) under 647 nm excitation at 15 K.

to that of *wt* amicyanin (Figure 7A) than to that of *wt* pseudoazurin.[44] The AmiPaz spectrum is dominated by intense transitions at 390 and 424 cm^{-1}, similar to *wt* amicyanin, and all of the vibrational frequencies above 360 cm^{-1} are within 1 cm^{-1} of those in *wt* amicyanin. In contrast, the intense Raman signals at 386, 397, and 444 cm^{-1} in *wt* pseudoazurin are not correlated to those in AmiPaz.

The Raman spectral pattern for *AmiAzu* (Figure 7D) is not as similar to *wt* amicyanin as is the case for AmiPcy and AmiPaz, but it still appears to be closer to that of *wt* amicyanin than to that of *wt* azurin.[45] Three of the major peaks at 369, 401, and 423 cm^{-1} in AmiAzu differ by 0, −3, and −2 cm^{-1}, respectively, from the peaks in *wt* amicyanin. The same peaks differ by −6, +3, and −8 cm^{-1}, respectively, from the signals in *wt* azurin.[45] The decrease in Raman frequencies as well as the increase in Raman intensities at 369 and 401 cm^{-1} in AmiAzu is indicative of a more tetragonal site than in *wt* amicyanin.

An intensity-weighted average of the Raman frequencies for the three most intense fundamentals reveals values of 402, 400, and 397 cm^{-1} for AmiPcy, AmiPaz, and AmiAzu, respectively (Table 2). These Cu−S(Cys) stretching frequencies are lower than the 409 cm^{-1} value in *wt* Ami and, thus, indicative of more rhombic type-1 structures[46] as has also been noted from the absorption and EPR spectra of the loop mutants.

(44) Han, J.; Adman, E. T.; Beppu, T.; Codd, R.; Freeman, H. C.; Huq, L.; Loehr, T.; Sanders-Loehr, J. *Biochemistry* **1991**, *30*, 10904−10913.

(45) den Blaauwen, T.; Hoitink, C. W.; Canters, G. W.; Han, J.; Loehr, T. M.; Sanders-Loehr, J. *J. Biochem.* **1993**, *32*, 12455−12464.

(46) Andrew, C. R.; Yeom, H.; Valentine, J. S.; Karlsson, B. G.; Bonander, N.; van Pouderoyen, G.; Canters, G. W.; Loehr, T. M.; Sanders-Loehr, J. *J. Am. Chem. Soc.* **1994**, *116*, 11489−11498.

Discussion

Loop-directed mutagenesis was used to study the influence of the C-terminal ligand-containing loop on the structure and reactivity of the active site of the cupredoxin amicyanin. The three loop mutants that are solely based on cupredoxins (AmiPcy, AmiAzu, and AmiPaz) have stable copper centers and are perfectly redox active proteins. The AmiNiR loop mutant, in which the ligand-containing loop of the type-1 copper site of a blue nitrite reductase has been introduced, is less stable and, therefore, only UV/vis and EPR spectroscopy have been used to characterize this protein.

The *EPR and UV/vis* spectra indicate that these loop mutants, with the exception of AmiNiR, have active sites which are more rhombic than that of *wt* amicyanin. The degree of rhombicity is smallest in AmiAzu with AmiPcy and AmiPaz being more rhombic. It is interesting to note that in the cases of AmiPaz and AmiAzu the $A_{\sim 460}/A_{\sim 600}$ ratio increases toward lower temperatures. The largest changes are observed between 298 and 220 K. These observations indicate that in some of the loop mutants the sites have acquired a plasticity that is absent in the natural sites, a feature that has been observed before for modified type-1 sites.[45,47]

The *reduction potentials* of the AmiAzu, AmiPaz, and AmiPcy are all higher than that of *wt* amicyanin. This could be due to a decrease in the solvent accessibility with increasing length of the ligand loop.[48,49] Alternatively, the loop mutants may be able to better accommodate the reduced copper ion. A similar conclusion has been drawn from studies on the Pro80Ile mutant of pseudoazurin.[50] NMR relaxation dispersion experiments are planned to probe the acessibility of the copper site in the protein variants.

The *self-exchange rate constants* of the loop mutants of amicyanin are all lower than the k_{ese} of *wt* amicyanin, but often larger than the ese rate of the protein from which the loop originates. The parameters that determine ET rates are (a) driving force, which is zero in our case, (b) the equilibrium constant, K_{ass}, for the formation of the association complex between the redox partners, (c) the reorganizational energy, λ, and (d) the electronic coupling between the redox centers, H_{AB}.[51] The order of magnitude decrease in k_{ese} of the loop mutants compared to *wt* amicyanin can be due to changes in any of the three latter parameters. A rough estimate shows that a decrease in the Gibbs free energy of association by 1.4 kcal/mol, an increase in distance between the reaction partners in the association complex by 0.7 Å, or an increase in the reorganization energy by 250 meV each in itself would be sufficient to account for an order of magnitude decrease in k_{ese}. These values are not unrealistic. For instance, the Gibbs free energy of association of two azurin molecules has been estimated as -1 to -2 kcal/mol;[47e] a change in the "roughness" of the surface patch that mediates ET in the blue copper proteins by 0.35 Å, which is a few tenths of the van der Waals radius of a H-atom, would increase the electronic coupling path length by 0.7 Å; finally, reorganizational energies of blue copper centers encompass a range of 0.5−1.5 eV[52] and a change by 250 meV still would leave the modified site within the range of blue copper centers.

The *protonation behavior* of the C-terminal histidine ligand in the reduced protein appears to be affected by the loop mutations. In AmiPcy, AmiAzu, and AmiPaz the loop mutation results in a decrease of the pK_a for this histidine with respect to native amicyanin. This means that at the temperature used in this study (25 °C), the histidines bind more strongly to the reduced copper in the loop variants than in the native amicyanin. It is conceivable that the non-native loops do not pack as well against the β-sandwich that forms the core of the protein structure as does the native loop in amicyanin. The non-native loops, thus, might retain some flexibility that would lead to a favorable entropic term for the formation of the Cu−His bond. Titration of C-terminal ligand histidines has been observed for native plastocyanins, amicyanins, and pseudoazurins, but is conspicuously absent in the azurins. It has been suggested[20] that this might be correlated with the composition of the C-terminal ligand loop, in particular the Cys-His stretch (4 intervening residues in the azurins, 2 in the other proteins). The present experiments show at least that the composition of the loop cannot be the only parameter that determines the protonation behavior of the C-terminal ligand histidine: the histidine in the AmiAzu variant clearly titrates. As already mentioned, the packing of the loop may play a role, but electrostatic interactions and solvent accessibility may affect the titration behavior also.

Mechanistic Features. The findings of the present and previous studies show that it is possible to alter the metal site to quite an extent, while preserving its type-1 character. The native ligand binding loop can be replaced by non-native loops without the protein losing its metal binding characteristics. As pointed out above, modifying the metal site leads to enhanced mobility of the protein matrix around the metal, a less well determined coordination geometry, and, sometimes, the occurrence of different metal coordination geometries in equilibrium with each other. This may affect the spectroscopic, structural, and dynamic properties of the metal site, but, evidently, the mechanistic (kinetic and thermodynamic) properties are not seriously compromised: the rate at which ET is catalyzed by the loop mutants remains high and the redox potential remains

(47) (a) Danielsen, E.; Bauer, R.; Hemmingsen, L.; Bjerrum, M. J.; Butz, T.; Troger, W.; Canters, G. W.; den Blaauwen, T.; van Pouderoyen, G. *Eur. J. Biochem.* **1995**, *233*, 554−560. (b) den Blaauwen, T.; van de Kamp, M.; Canters, G. W. *J. Am. Chem. Soc.* **1991**, *113*, 5050−5052. (c) den Blaauwen, T.; Canters, G. W. *J. Am. Chem. Soc.* **1993**, *115*, 1121−1129. (d) van Pouderoyen, G.; den Blaauwen, T.; Reedijk, J.; Canters, G. W. *Biochemistry* **1996**, *35*, 13205−13211. (e) van Pouderoyen, G.; Andrew, C. R.; Loehr, T. M.; Sanders-Loehr, J.; Mazumdar, S.; Allen, H.; Hill, H. A. O.; Canters, G. W. *Biochemistry* **1996**, *35*, 1397−1407. (f) Regan, J. J.; DiBilio, A. J.; Winkler, J. R.; Richards, J. H.; Gray, H. B. *Inorg. Chim. Acta* **1998**, *276*, 470−480. (g) Vila, A. J.; Ramirez, B. E.; DiBilio, A. J.; Mizoguchi, T. J.; Richard, J. H.; Gray, H. B. *Inorg. Chem.* **1997**, *36*, 4567−4570. (h) Germanas, J. P.; DiBilio, A. J.; Gray, H. B.; Richards, J. H. *Biochemistry* **1993**, *32*, 7698−7702. (i) Danielsen, E.; Kroes, S. J.; Canters, G. W.; Hemmingsen, L.; Singh, K.; Messerschmidt, A. *Eur. J. Biochem.* **1997**, *250*, 249−259. (j) Kroes, S. J.; Hoitink, C. G.; Andrew, C. R.; Ai, J. Y.; Sanders-Loehr, J.; Messerschmidt, A.; Hagen, W. R.; Canters, G. W. *Eur. J. Biochem.* **1996**, *240*, 342−351. (k) Salgado, J.; Jimenez, H. R.; Moratal, J. M.; Kroes, S.; Warmerdam, G. W.; Canters, G. W. *Biochemistry* **1996**, *35*, 1810−1819. (l) Salgado, J.; Kroes, S. J.; Berg, A.; Moratal, J. M.; Canters, G. W. *J. Biol. Chem.* **1998**, *273*, 177−185. (m) Bonander, N.; Karlsson, B. G.; Vanngard, R. *Biochemistry* **1996**, *35*, 2429−2436. (n) Strange, R. W.; Murphy, L. M.; Karlsson, B. G.; Reinhammar, B.; Hasnain, S. S. *Biochemistry* **1996**, *35*, 16391−16398. (o) Karlsson, B. G.; Tsai, L. C.; Nar, H.; Sanders-Loehr, J.; Bonander, N.; Langer, V.; Sjolin, L. *Biochemistry* **1997**, *36*, 6-4089−4095. (p) Hammann, C.; van Pouderoyen, G.; Nar, H.; Gomis, R. F.; Messerschmidt, A.; Huber, R.; den Blaauwen, T.; Canters, G. W. *J. Mol. Biol.* **1997**, *266*, 357−366. (q) Messerschmidt, A.; Prade, L.; Kroes, S. J.; Sanders-Loehr, J.; Huber, R.; Canters, G. W. *Proc. Natl. Acad. Sci. U.S.A.* **1998**, *95*, 3443−3448.

(48) Churg, A. K.; Warshel, A. *Biochemistry* **1986**, *25*, 1675−1681.

(49) DiBilio, A. J.; Chang, T. K.; Malmström, B. G.; Gray, H. B.; Karlsson, B. G.; Nordling, M.; Pascher, T.; Lundberg, L. G. *Inorg. Chim. Acta* **1992**, *198*−*200*, 145−148.

(50) Libeu, C. A. P.; Kukimoto, M.; Nishiyama, M.; Horinouchi, S.; Adman, E. T. *Biochemistry* **1997**, *36*, 13160−13179.

(51) Canters, G. W.; Dennison, C. *Biochimie* **1995**, *77*, 506−515.

(52) (a) Farver, O.; Skov, L. K.; Gilardi, G.; van Pouderoyen, G.; Canters, G. W.; Wherland, S.; Pecht, I. *Chem. Phys.* **1996**, *204*, 271−277. (b) DiBilio, A. J.; Dennison, C.; Gray, H. B.; Ramirez, B. E.; Sykes, A. G.; Winkler, J. R. *J. Am. Chem. Soc.* **1998**, *120*, 7551−7556.

within the customary range of redox potentials of blue copper proteins. These findings seem to disprove the idea, elaborated on in the Introduction, that in the blue copper proteins the protein conformation is unique ("entatic"; "rack" character) in the sense that it has a conformation that ensures high ET rates and proper tuning of the redox potential. This might also explain why, in the course of evolution, the combination of the cupredoxin fold and type-1 copper site has been such a successful alternative for the c-type cytochromes. An important part of the Cu coordination sphere is provided by the ligand loop. The present work shows that the details of the loop do not seem to matter so much as far as the mechanistic properties of the cupredoxin are concerned. As long as the loop contains the three canonical ligands it will form a viable type-1 site. This is somewhat reminiscent of the $[Fe_4-S_4]$-clusters in iron−sulfur proteins in which the cysteine ligands are located on a single loop. Provided this loop is grafted onto a stable framework, the Fe−S cluster can assemble spontaneously in the presence of inorganic sulfide.[53]

Type-1 Site Structure. In one respect the idea of a "loop" containing three ligands needs refinement. Two of the ligands occur at the transition from β-sandwich to loop, i.e., the cysteine and the methionine. Although their side chain conformations may be sensitive to the overall loop conformation, their backbones are firmly anchored to the β-sandwich. Thus the β-sandwich provides an important structural constraint for the copper site. This becomes evident from the RR spectra: for the loop mutants in the present study the RR spectrum, which is dominated by the Cu−Cys interaction, looks more like the spectrum of native amicyanin than like the spectra of the proteins from which the loops originate. The only really variable elements of the ligand loop appear to be its length and the position of the C-terminal histidine. Although it is considered as one of the three strong ligands of the copper, this histidine often dissociates when the metal is reduced at low pH (<7). This even holds to some extent for the azurins: when the structural constraints on the C-terminal histidine in azurin are relaxed by severing the $C^{\alpha}-C^{\beta}$ bond of His117, the imidazole drops out of the protein structure upon reduction of the copper. Thus, contrary to what is often suggested, the metal binding site of the cupredoxins seems to be tailored to stabilize copper in its oxidized instead of its reduced form. A similar conclusion based on GuHCl-induced unfolding experiments of azurin was reached by the Pasadena and Göteborg groups.[54] This also explains the ease by which the C-terminal histidine ligand can be excised and replaced by external ligands without losing the metal binding property of the protein.[47b,c]

Conclusion

In conclusion it can be stated that the combination of a β-sandwich and a ligand loop, with two of the ligands anchored at the rim of the sandwich structure, provides a versatile framework for binding a copper ion and for creating an effective and efficient ET center. The protein core acts as a bowl or a setting for the copper ion and the ligand loop closes it off like a lid. One strong ligand (the N-terminal histidine) is located inside the protein core, one is located on the loop (the N-terminal histidine), and the two S-donor ligands (the cysteine and the methionine) are found at the transition from core to loop and provide the anchor points for the lid. It is well-known that the histidine ligand in this loop acts as the gate by which electrons enter and leave the active site.[1] In fact this histidine is part of the surface patch by which blue copper proteins associate with their redox partners.[55−59] From inspection of the 3D structures of blue copper proteins it is evident that the ligand loop folds closely around this histidine. The variability of this loop thus may provide a unique evolutionary window to engineer specificity for partner recognition without jeopardizing the ET function of the protein.

Acknowledgment. This work was supported in part by the Foundation for Chemical Research (SON) under the auspices of The Netherlands Science Organisation (NWO), by the Dutch Association of Biotechnological Research Schools (ABON), and by the National Institutes of Health (GM 18865). Generous financial support by the German Science Foundation (DFG), the Volkswagenstiftung, the DAAD, and the NWO is gratefully acknowledged, as is the assistance of Jingyuan Ai, Linda Cameron, and Frederik Rotsaert for their assistance with the Raman experiments.

JA992796B

(53) (a) Gibrey, B. R.; Mulholland, S. E.; Rabenal, F.; Dutton, S. L. *Proc. Natl. Acad. Sci. U.S.A.* **1996**, *93*, 15041−15046. (b) Mulholland, S. E.; Gibrey, B. R.; Rabenal, F.; Dutton, P. L. *J. Am. Chem. Soc.* **1998**, *120*, 10296−10302.

(54) (a) Winkler, J. R.; Wittung-Stafhede, P.; Leckner, J.; Malmström, B. G.; Gray, H. B. *Proc. Natl. Acad. Sci. U.S.A.* **1997**, *94*, 4246−4249. (b) Wittung-Stafhede, P.; Hill, M. G.; Gomez, E.; Di Bilio, A. J.; Karlsson, B. G.; Leckner, J.; Winkler, J. R.; Gray, H. B.; Malmström, B. G. *J. Biol. Inorg. Chem.* **1998**, *3*, 367−370.

(55) Chen, L.; Durley, R.; Poliks, B. J.; Hamada, K.; Chen, Z.; Mathews, F. S.; Davidson, J. L.; Satow, Y.; Huizinga, E.; Vellieux, F. M. D.; Hol, W. G. J. *Biochemistry* **1992**, *31*, 4959−4964.

(56) Brooks, H. B.; Davidson, V. L. *Biochemistry* **1994**, *33*, 5696−5701.

(57) Ubbink, M.; Ejdeback, M.; Karlsson, B. G.; Bendall, D. S. *Structure* **1998**, *6*, 323−335.

(58) Kukimoto, M.; Nishiyama, M.; Ohnuki, T.; Turley, S.; Adman, E. T.; Horinouchi, S.; Beppu, T. *Protein Eng.* **1995**, *8*, 153−158.

(59) van Pouderoyen, G.; Mazumdar, S.; Hunt, N. I.; Hill, H. A. O.; Canters, G. W. *Eur. J. Biochem.* **1994**, *222*, 583−588.

(60) van Houwelingen, T.; Canters, G. W.; Stobbelaar, G.; Duine, J. A.; Frank, J.; Tsugita, A. *Eur. J. Biochem.* **1985**, *153*, 75−80.

(61) Sykes, A. G. *Struct. Bonding* **1990**, *75*, 175−224.

(62) Reference deleted in press.

(63) Reference deleted in press.

(64) van de Kamp, M.; Silvestrini, M. C.; Brunori, M.; van Beeumen, J.; Hali, F. C.; Canters, G. C. *Eur. J. Biochem.* **1990**, *194*, 109−118.

(65) van de Kamp, M.; Canters, G. W.; Andrew, C. R.; Sanders-Loehr, J.; Bender, C. J.; Peisach, J. *Eur. J. Biochem.* **1993**, *218*, 229−238.

(66) Groeneveld, M.; Aasa, R.; Reinhammer, B.; Canters, G. W. *J. Inorg. Biochem.* **1987**, *31*, 143−154.

(67) Kohzuma, T.; Dennison, C.; McFarlane, W.; Nakashimal, S.; Kitagawa, T.; Inoue, T.; Kai, Y.; Nishio, N.; Shidara, S.; Suzuki, S.; Sykes, G. *J. Biol. Chem.* **1995**, *270*, 25733−25738.

(68) Dennison, C.; Kohzuma, T.; McFarlane, W.; Suzuki, S.; Sykes, A. G. *J. Chem. Soc., Dalton Trans.* **1994**, 437−443.

(69) Zumft, P.; Gotzmann, D. J.; Kroneck, P. M. H. *Eur. J. Biochem.* **1987**, *168*, 301−307.

(70) Kukimoto, M.; Nishiyama, M.; Murphy, M. E. P.; Turley, S.; Adman, E. T.; Horinouchi, S.; Beppu, T. *Biochemistry* **1994**, *33*, 5246−5252.